medRxiv preprint doi: https://doi.org/10.1101/2023.08.07.23293304; this version posted May 10, 2024. The copyright holder for this preprint (which was not certified by peer review) is the author/funder, who has granted medRxiv a license to display the preprint in perpetuity. It is made available under a CC-BY-NC-ND 4.0 International license .

High-throughput detection of neutralizing antibodies to SARS-CoV-2 variants using flow cytometry

Running Head: High-throughput broad SARS-CoV-2 variants neutralizing assay

Xiaohan Zhang[1,2*], Yajie Wang[3*], Mansheng Li[1*], Haolong Li[4*], Xiaomei Zhang[1], Xingming Xu[1], Di Hu[5], Te Liang[1], Yunping Zhu[1], Yongzhe Li[4#], Bingwei Wang[2#] and Xiaobo Yu[1,6#]

Affiliations

[1]State Key Laboratory of Medical Proteomics, Beijing Proteome Research Center, National Center for Protein Sciences-Beijing (PHOENIX Center), Beijing Institute of Lifeomics, Beijing, 102206, China.

[2]School of Medicine, Nanjing University of Chinese Medicine, Nanjing 210023, China.

[3]Department of Clinical Laboratory, Beijing Ditan Hospital, Capital Medical University, Beijing 100015, China.

[4]Department of Clinical Laboratory, Peking Union Medical College Hospital, Chinese Academy of Medical Science & Peking Union Medical College, Beijing 100730, China.

NOTE: This preprint reports new research that has not been certified by peer review and should not be used to guide clinical practice.

medRxiv preprint doi: https://doi.org/10.1101/2023.08.07.23293304; this version posted May 10, 2024. The copyright holder for this preprint (which was not certified by peer review) is the author/funder, who has granted medRxiv a license to display the preprint in perpetuity. It is made available under a CC-BY-NC-ND 4.0 International license .

[5]ProteomicsEra Medical Co., Ltd., Beijing, 102206, China

[6]The First Affiliated Hospital of Wenzhou Medical University, Wenzhou, China.

[*]These authors contributed equally to this work.

[#]Correspondence to xiaobo.yu@hotmail.com (X.Y.), bingweiwang@njucm.edu.cn (B.W.) and yongzhelipumch@126.com (Y. L).

medRxiv preprint doi: https://doi.org/10.1101/2023.08.07.23293304; this version posted May 10, 2024. The copyright holder for this preprint (which was not certified by peer review) is the author/funder, who has granted medRxiv a license to display the preprint in perpetuity. It is made available under a CC-BY-NC-ND 4.0 International license .

Abstract

Detecting neutralizing antibodies (NAbs) to SARS-CoV-2 variants is crucial for controlling COVID-19 spread. We developed a high-throughput assay for the broad systematic examination of NAbs to eleven SARS-CoV-2 variants, which include D614G, Alpha, Beta, Gamma, Delta, Kappa, and Omicron sub-lineages BA.1-BA.5. The assay is cost-effective, reliable, 35-fold more sensitive than Luminex technology, and can include new variants during SARS-CoV-2 evolution. Importantly, our results highly correlated with a commercial IgG serological assay (R = 0.89) , the FDA-approved cPass sVNT assay (R = 0.93), pseudivirus-based neutralizing assay (R = 0.96, R = 0.66, R = 0.65) and live virus based neutralization assay (R = 0.79, R = 0.64) . Using this platform, we constructed a comprehensive overview of the interactions between SARS-CoV-2 variants' Spike trimer proteins and ACE2 receptors, and identified a polyclonal Ab with broad neutralizing activity. Furthermore, when compared to the D614G variant, we found that the serum NAbs elicited by the third dose vaccine demonstrated decreased inhibition to multiple SARS-CoV-2 variants, including Gamma (0.94×), Alpha (0.91×), Delta (0.91×), Beta (0.81×), Kappa (0.81×), BA.2 (0.44×), BA.1 (0.43×), BA.3 (0.41×), BA.5 (0.35×) and BA.4 (0.33×), in cohort of 56 vaccinated individuals. Altogether, our proteomics platform proves to be an effective tool to

medRxiv preprint doi: https://doi.org/10.1101/2023.08.07.23293304; this version posted May 10, 2024. The copyright holder for this preprint (which was not certified by peer review) is the author/funder, who has granted medRxiv a license to display the preprint in perpetuity. It is made available under a CC-BY-NC-ND 4.0 International license .

detect broad NAbs in the population and aid in the development of future COVID-19 vaccines and vaccination strategies.

Keywords

SARS-CoV-2, flow cytometry, neutralization, antibody, COVID-19

medRxiv preprint doi: https://doi.org/10.1101/2023.08.07.23293304; this version posted May 10, 2024. The copyright holder for this preprint (which was not certified by peer review) is the author/funder, who has granted medRxiv a license to display the preprint in perpetuity. It is made available under a CC-BY-NC-ND 4.0 International license .

Introduction

The ongoing coronavirus 2019 (COVID-19) pandemic, caused by the severe acute respiratory syndrome coronavirus 2 (SARS-CoV-2), remains a public health concern worldwide. This is primarily attributed to the continuous evolution of the virus and its persistent transmission across global populations[1]. For instance, over ten SARS-CoV-2 variants of concern (VOCs) have appeared, and these VOCs have the potential to reduce the immune response[2]. According to reports, 17.13% (95%CI, 7.55–26.71%) of asymptomatic infected individuals may have long-term health consequences[3], which may include symptoms such as fatigue, brain fog, dizziness, gastrointestinal symptoms, as well as others[4].

Neutralizing antibodies (NAbs) of SARS-CoV-2 are a subset of antibodies that block viral entry by inhibiting the interaction between the SARS-CoV-2's surface protein, Spike, and the host cell's receptor, angiotensin-converting enzyme 2 (ACE2). Such NAbs can be produced following COVID-19 vaccination or SARS-CoV-2 infection. Identifying SAR-CoV-2 NAbs is critical for assessing vaccine efficacy, evaluating individual and population immunity, monitoring variant susceptibility, and information public health measures to control the spread of COVID-19. However, traditional methods of NAb detection, such those that use a live virus or a pseudovirus-based neutralization

medRxiv preprint doi: https://doi.org/10.1101/2023.08.07.23293304; this version posted May 10, 2024. The copyright holder for this preprint (which was not certified by peer review) is the author/funder, who has granted medRxiv a license to display the preprint in perpetuity. It is made available under a CC-BY-NC-ND 4.0 International license .

assay, are slow, expensive, carry a potential risk of infection, and may require specialized biosafety level 3 (BSL3) facilities [5-8].

As an alternative approach, enzyme-linked immunosorbent assay (ELISA) can perform the *in vitro* neutralizing testing using purified Spike, ACE2, or Spike's receptor-binding domain (RBD) that interacts directly with ACE2 during viral entry. Several commercial ELISA-based surrogate virus neutralization tests (sVNT) have been developed, including TECO sVNT (TECO Medical) and cPASS sVNT (GenScript), which have been approved by the United States' (U.S.) Food and Drug Administration (FDA) or received Conformite Europeenne (CE) marking for use in the European Union [9,10]. Unfortunately, ELISA-based methods only detect a single variant at a time, making them a time-consuming option when multiple SARS-CoV-2 variants are analyzed [6].

To address this concern, Fenwick *et al.* developed a multiplexed *in-vitro* quantitative neutralization assay using Luminex technology in 2021. The assay enables the detection of NAbs targeting various Spike mutations, including D614G, D614G plus M153T, N439K, S477N, S477R, E484K, S459Y, N501T, N501Y, K417N, 60-70, P681H, Y453F, and their combinations. The results obtained from this assay correlated with pseudovirus neutralization (R^2=0.65) and live virus infection (R^2 = 0.825) assays [7].

medRxiv preprint doi: https://doi.org/10.1101/2023.08.07.23293304; this version posted May 10, 2024. The copyright holder for this preprint (which was not certified by peer review) is the author/funder, who has granted medRxiv a license to display the preprint in perpetuity. It is made available under a CC-BY-NC-ND 4.0 International license .

In a similar vein, Lynch et al. developed a multiplexed surrogate virus neutralization test (plex-sVNT) for detecting NAbs to seven SARS-CoV-2 variants, namely, wild type, Alpha, Beta, Gamma, Delta, Kappa, and Epsilon. The results highly correlated (> 96%) with those obtained from a plaque reduction neutralization test (PRNT)[8].

However, it should be noted that these technologies have limitations as they require access to specific Luminex and Bio-Rad instruments, thereby restricting their use to specific laboratories. Moreover, some recent Omicron variants have not been accessible for analysis using these methods to date[11].

In this work, we developed a high-throughput broad neutralizing antibody (bNAb) assay that enables the systematic detection of NAbs to eleven SARS-CoV-2 VOCs that is reliable, cost-effective, sensitive, and used with a standard flow cytometer [12]. These variants include D614G, Alpha, Beta, Gamma, Delta, Kappa, Omicron BA.1, Omicron BA.2, Omicron BA.3, Omicron BA.4, and Omicron BA.5. We conducted a comparative analysis of NAb detection using our SARS-CoV-2 bNAb assay with commercial ELISA-based serology, U.S. FDA-approved cPASS sVNT, pseudivirus-based neutralizing assays and live virus based neutralization assay. Furthermore, we explored the applications of the SARS-CoV-2 bNAb assay for screening therapeutic Abs, assessing their neutralizing activity SARS-CoV-2. Finally, we analyzed

medRxiv preprint doi: https://doi.org/10.1101/2023.08.07.23293304; this version posted May 10, 2024. The copyright holder for this preprint (which was not certified by peer review) is the author/funder, who has granted medRxiv a license to display the preprint in perpetuity. It is made available under a CC-BY-NC-ND 4.0 International license .

the broad responses of serological NAbs to SARS-CoV-2 variants in individuals who received the third dose of either the inactivated vaccine (Sinovac-CoronaVac) or the recombinant subunit vaccine (ZF2001) for COVID-19.

Results

Schematic illustration of SARS-CoV-2 bNAb assay

In the SARS-COV-2 bNAb assay, illustrated schematically in Figure 1A, the trimerized Spike proteins of six non-Omicron variants (D614G, Alpha, Beta, Kappa, Gamma, Delta) and five Omicron variants (BA.1, BA.2, BA.3, BA.4, BA.5) were expressed from human embryonic kidney 293 (HEK293) cells, purified, and coupled to the magnetic-fluorescent beads, as previously reported [7,13]. During the NAbs detection process, all coupled beads were mixed together and incubated with samples containing NAbs. The NAbs bound to the Spike trimer proteins, preventing their interaction with the biotinylated ACE2 receptors, which were coupled to streptavidin-phycoerythrin (SA-PE). The inhibition rate (%) was calculated as follows: Inhibition rate (%) = (1 - signal of NAb inhibition on Spike-ACE2 binding / signal of Spike-ACE2 binding) × 100%.

The sensitive detection of Spike-ACE2 interactions is essential for assessing the presence of NAbs in clinical samples. To address this

medRxiv preprint doi: https://doi.org/10.1101/2023.08.07.23293304; this version posted May 10, 2024. The copyright holder for this preprint (which was not certified by peer review) is the author/funder, who has granted medRxiv a license to display the preprint in perpetuity. It is made available under a CC-BY-NC-ND 4.0 International license .

requirement, we coupled the Spike protein from six SARS-CoV-2 variants (D614G, Alpha, Beta, Kappa, Delta, Omicron BA.1) onto magnetic-fluorescent beads from Luminex and Shenzhen Wellgrow Technology Co., Ltd. ("Wellgrow"), and then incubated with different concentrations of ACE2. Magnetic-fluorescent beads with the SARS-CoV-2 nucleocapsid (N) protein, rather than the Spike protein, was employed as the negative control. The binding signals were measured using Luminex-200 and Wellgrow flow cytometry. Notably, the fluorescent signal intensity and signal to noise ratio (SNR) were much higher with the Wellgrow platform than the Luminex platform when ACE2 concentrations ranged from 0.01 μg/mL to 100 μg/mL (Figure 1B, Figure S1 and Table S6).

Furthermore, we calculated the sensitivity or the lowest detection limit (LOD) of each method, in which the LOD was equal to the signal of the buffer control plus ten standard deviations (Figure 1C). The data showed that the average LOD of our assay using the Wellgrow platform was 35.89±57.8 [-21.91~93.69]-fold higher than the Luminex platform for all variants (D614G, Alpha, Beta, Kappa, Delta, Omicron BA.1).

At last, we compared the difference of NAb titers obtained by detecting the inhibition of antibody #26 to Spike-ACE2 interaction. The results showed that the IC50 obtained by two platforms are highly

medRxiv preprint doi: https://doi.org/10.1101/2023.08.07.23293304; this version posted May 10, 2024. The copyright holder for this preprint (which was not certified by peer review) is the author/funder, who has granted medRxiv a license to display the preprint in perpetuity. It is made available under a CC-BY-NC-ND 4.0 International license .

consistence with the r correlation of 0.9988 (Figure S1D). Therefore, we chose the Wellgrow platform as the proteomics platform for the SARS-CoV-2 bNAb assay in this study.

Mapping Spike-ACE2 interactions of SARS-CoV-2 variants

Using our platform, we conducted a systematic investigation of the interactions between ACE2 and Spike trimer proteins from eleven SARS-CoV-2 variants. This was achieved by incubating a bead array with different concentrations of ACE2 (Figure 2). The results demonstrated that the fluorescent signals from the Spike trimer proteins increased with increasing concentrations of ACE2, indicating the formation of Spike-ACE2 complexes on the beads (Figure 2A).

Spike mutations were found to influence the interaction dynamics. At the maximal concentration of 10 μg/mL ACE2, Alpha and Delta variants exhibited the highest signals, followed by Beta, BA.4, BA.5, D614G, Gamma, BA.1, BA.2, and Kappa, with BA.3 showing the lowest signal. In contrast, the N protein, used as a negative control, consistently displayed the lowest signal regardless of ACE2 concentration.

To further assess the binding affinity, we calculated the half-maximal effective concentration (EC50) using the standard curve for each SARS-CoV-2 variant (Figure 2B). The results showed that

medRxiv preprint doi: https://doi.org/10.1101/2023.08.07.23293304; this version posted May 10, 2024. The copyright holder for this preprint (which was not certified by peer review) is the author/funder, who has granted medRxiv a license to display the preprint in perpetuity. It is made available under a CC-BY-NC-ND 4.0 International license .

Omicron BA.1 has the highest binding affinity with an EC50 of 0.2913 µg/mL, followed by Beta (0.2913 µg/mL), Delta (0.3415 µg/mL), Omicron BA.4 (0.3592 µg/mL), Gamma (0.3833 µg/mL), Alpha (0.394 µg/mL), Kappa (0.3983 µg/mL), Omicron BA. 2 (0.4307µg/mL), Omicron BA. 5(0.4593 µg/mL), D614G (0.5279 µg/mL), and Omicron BA.3 (1.283 µg/mL). The results are in accordance with surface plasma resonance data in which BA.1 has the strongest interaction with ACE2 with a dissociation constant (K_D) of 2.10 nM, followed by BA.2 (2.21 nM) and D614G (5.20 nM) [14]. Similar results were obtained by Mahalingam et al., who used ELISA to determine the EC50 of ACE2 to Spike Omicron (0.38 nM), Delta (0.48 nM), and wild type (2.28 nM)[15]. Collectively, our data provide a comprehensive landscape of Spike trimer-ACE2 interactions for SARS-CoV-2 VOCs, as classified by the U.S. Centers for Disease Control and Prevention (CDC) (https://www.cdc.gov/coronavirus/2019-ncov/variants/variant-classifications.html). It should be noted that the Epsilon variant was not included in this work due to the unavailability of purified Spike trimer protein at the time of executing experiments.

In addition, to demonstrate the specificity of our assay, we tested the binding ability of ACE2 to the Spike proteins from MERS, SARS-CoV and six SARS-CoV-2 variants. The results showed that the binding signal of ACE2 to six SARS-CoV-2 variant Spike proteins was

medRxiv preprint doi: https://doi.org/10.1101/2023.08.07.23293304; this version posted May 10, 2024. The copyright holder for this preprint (which was not certified by peer review) is the author/funder, who has granted medRxiv a license to display the preprint in perpetuity. It is made available under a CC-BY-NC-ND 4.0 International license .

much higher than that of SARS-CoV and MERS. The binding signal of SARS-CoV was 3.38-5.74 times lower than that of SARS-CoV-2 variants, due to the homology of Spike sequence. There was no binding signal observed between ACE2 and MERS, similar to the negative control, N protein (Figure S2). All these results are accord to the reported results[16], and demonstrate our assay is specific.

Comparison of SARS-CoV-2 bNAb assay to ELISA , cPass sVNT, pseudovirus-based neutralization and live virus based neutralization assays.

To assess the reliability of the SARS-CoV-2 bNAb assay, we compared the SARS-CoV-2 bNAb assay to an ELISA that was used to detect anti-Spike IgG antibodies[17]. The results showed a high correlation between the levels of D614G NAbs detected using our SARS-CoV-2 bNAb assay and the anti-Spike IgG antibodies obtained by the ELISA [R = 0.89, p-value (p) < 2.2 e-16] in a cohort of 75 individuals (Figure 3A).

Next, we compared the NAb results obtained from the SARS-CoV-2 bNAb assay to those obtained from the FDA-approved cPass sVNT test [6,9]. The data obtained using the SARS-CoV-2 bNAb assay and cPass sVNT test demonstrated a higher correlation to each other (R = 0.93, p < 2.2 e-16) compared to the assay using Luminex

medRxiv preprint doi: https://doi.org/10.1101/2023.08.07.23293304; this version posted May 10, 2024. The copyright holder for this preprint (which was not certified by peer review) is the author/funder, who has granted medRxiv a license to display the preprint in perpetuity. It is made available under a CC-BY-NC-ND 4.0 International license .

technology (R = 0.85)[18]. The positive percent agreement (PPA) was 92.7% (80.1%-98.5%) and the negative percent agreement (NPA) was 94.1% (80.3%-99.3%) (Figure 3B). The findings suggest that some of the anti-Spike IgG antibodies detected by the ELISA may lack neutralizing activity and therefore were not detected by SARS-CoV-2 bNAb assay[19]. Overall, these results demonstrate the reliability of the SARS-CoV-2 bNAb assay as an *in vitro* platform for detecting serum NAbs.

Additionally, we compared the inhibition rate (%) of NAbs obtained by SARS-CoV-2 bNAb assay to the NAb titers obtained by pseudovirus-based neutralization assay or live virus based neutralization assay. For 10 serum samples from mice administered with WT mRNA vaccines, a high correlation was found between D614G NAbs inhibition rate (%) detected using SARS-CoV-2 bNAb assay and WT NAb titers by pseudovirus-based neutralization assay (R = 0.96, $p < 0.0001$) and live virus based neutralization assay (R = 0.79, $p < 0.0001$) (Figures 3C, 3E). Similarly, for 10 serum samples from mice administered with BA.1 mRNA vaccines, notable correlations were observed between the levels of BA.1 NAbs detected using SARS-CoV-2 bNAb assay and pseudovirus-based neutralization (R = 0.66, p = 0.0017) and live virus based neutralization assays (R = 0.64, p = 0.0022) (Figures 3D, 3F). Then, we compared the inhibition rate (%)

medRxiv preprint doi: https://doi.org/10.1101/2023.08.07.23293304; this version posted May 10, 2024. The copyright holder for this preprint (which was not certified by peer review) is the author/funder, who has granted medRxiv a license to display the preprint in perpetuity. It is made available under a CC-BY-NC-ND 4.0 International license .

of NAbs obtained by SARS-CoV-2 bNAb assay and the NAb titers obtained by pseudovirus-based neutralization assay in the serum of 135 individuals with second dose vaccination. We detected serum NAbs against the D614G variant using both assays. The results showed a correlation coefficient (r) of 0.65, demonstrating the consistency between the results obtained through inhibition and those obtained with NAb titers (Figure S4 and Table S7).

Identification of broadly neutralizing monoclonal/polyclonal Abs against SARS-CoV-2 variants

To demonstrate the application of SARS-CoV-2 bNAb assay in identifying monoclonal/polyclonal NAbs for potential treatment purposes, we tested six anti-Spike antibodies that are available in the laboratory[20] (Figure 4A). The results revealed that three antibodies (#26, #20, #21) have neutralizing activity. Antibodies #20 and #21 inhibited ACE2 binding to D614G, Alpha, Beta, Kappa and Delta variants, but were not effective in inhibiting the ACE2 binding to the Omicron BA.1 variant. Antibody #26 exhibited the ability to inhibit Spike-ACE2 interactions for D614G, Alpha, Beta, Kappa,Delta and Omicron BA.1 variants.

Subsequently, the half-maximal inhibitory concentration (IC50) values were calculated and represented in a heatmap (Figure 4B). The

medRxiv preprint doi: https://doi.org/10.1101/2023.08.07.23293304; this version posted May 10, 2024. The copyright holder for this preprint (which was not certified by peer review) is the author/funder, who has granted medRxiv a license to display the preprint in perpetuity. It is made available under a CC-BY-NC-ND 4.0 International license .

results showed that antibody #26 possessed broad neutralizing activity to all tested SARS-CoV-2 variants (Kappa, D614G, Alpha, Delta, Beta, Omicron BA.1). The IC50 to D614G (0.47 µg/mL) was confirmed with ELISA (0.35 µg/mL) and pseudovirus neutralizing assay (0.21 µg/mL) in our previous work[20]. While the IC50 of antibody #26 to the Omicron variant was ten-fold lower than non-Omicron variants. These findings underscore the ability of our assay to rapidly screen for monoclonal/polyclonal NAbs with potential therapeutic applications.

Evaluation of serum NAbs in individuals receiving the third dose vaccination

We tested the serum NAbs from 56 individuals who received two doses of the inactivated vaccine (Sinovac-CoronaVac) and boosted with a third dose with either an inactivated vaccine or recombinant subunit vaccine (ZF2001) (Table 1)[21]. The inhibition rate (%) was calculated by deducting the background noise using 147 serum samples collected prior to the COVID-19 pandemic[22]. The results showed that the third dose vaccination elicited a strong protective immune response against the non-Omicron variants with the highest inhibition rate (%) of D614G, followed by Gamma, Alpha, Delta, and Kappa variants. Unfortunately, the inhibition rate (%) was much lower in Omicron BA.2 (0.44×), BA.1 (0.43×), BA.3 (0.41×), BA.5 (0.35×), and BA.4 (0.33×) variants,

medRxiv preprint doi: https://doi.org/10.1101/2023.08.07.23293304; this version posted May 10, 2024. The copyright holder for this preprint (which was not certified by peer review) is the author/funder, who has granted medRxiv a license to display the preprint in perpetuity. It is made available under a CC-BY-NC-ND 4.0 International license .

indicating the resistance of these variants to the Sinovac-CoronaVac vaccine and the ZF2001 vaccine (Figure 5A).

Next, we compared the inhibition (%) of serum NAbs in individuals who received either a third dose of inactivated vaccine or recombinant vaccine; no significant difference was observed (Figure 5B). These findings highlight the immunological resistance of different SARS-CoV-2 variants to the Sinovac-CoronaVac and ZF2001 vaccines, and suggest the need for developing a new vaccine that provides broad protection against SARS-CoV-2 variants.

Furthermore in order to demonstrate the specificity of our SARS-CoV-2 bNAb assay, we detected the serum from the individuals before vaccination (n = 147) and after three-dose vaccination (n = 56). The results showed that the serum NAb levels were significantly higher in the vaccination group than un-vaccination group ($p < 0.0001$) (Figure S3), indicating our SARS-CoV-2 bNAb assay is highly specific for the detection of serum NAbs.

Discussion

Even though the World Health Organization has announced that COVID-19 is no longer a public health emergency of international concern, the genome sequence of SARS-CoV-2 is continually evolving and the new variants (i.e. EG.5) may has the potential to escape the

medRxiv preprint doi: https://doi.org/10.1101/2023.08.07.23293304; this version posted May 10, 2024. The copyright holder for this preprint (which was not certified by peer review) is the author/funder, who has granted medRxiv a license to display the preprint in perpetuity. It is made available under a CC-BY-NC-ND 4.0 International license .

immunity and threat the people's health, especially among immunocompromised individuals[23,24]. Therefore, there is still a need for effective COVID-19 vaccines to prevent and control viral transmission. The development and deployment of vaccines for COVID-19, as well as the evaluation of population immunity, remain important for public health[25].

In this work, we developed a high-throughput SARS-CoV-2 bNAb assay to detect a wide range of NAbs to non-Omicron and Omicron variants. Compared to the assay using Luminex technology[7,8], our SARS-CoV-2 bNAb assay is 35-fold more sensitive, 2.5-fold less costly, and can be accessible to any laboratory that has a standard flow cytometer with the 532 nm and 635 nm lasers. Moreover, the simultaneous detection of NAbs to multiple SARS-CoV-2 variants can be achieved within a single experiment, and the assay can be periodically updated to include new variants. The reliability of NAb detection using our SARS-CoV-2 bNAb assay is demonstrated through comparisons with ELISA-based IgG serology, the cPass sVNT assay, pseudovirus-based neutralization assay and live virus based neutralization assay (Figure 3).

Using this platform, we constructed a comprehensive landscape of Spike trimer and ACE2 interactions for eleven SARS-CoV-2 variants (Figure 2). The results provide evidence that Omicron BA.1 showed the

medRxiv preprint doi: https://doi.org/10.1101/2023.08.07.23293304; this version posted May 10, 2024. The copyright holder for this preprint (which was not certified by peer review) is the author/funder, who has granted medRxiv a license to display the preprint in perpetuity. It is made available under a CC-BY-NC-ND 4.0 International license .

strongest binding affinity to the ACE2 receptor [26,27]. Notably, the transmission rate of SARS-CoV-2 and its variants is dependent on numerous factors, including immune resistance, toxicity, etc[28].

Furthermore, our investigation of serum NAbs in vaccinated individuals showed that the third dose of the inactivated vaccine or recombinant RBD vaccine resulted in a strong inhibition of Spike-ACE2 interactions to the non-Omicron variants (D614G, Alpha, Beta, Gamma, Kappa). However, the protection was significantly decreased for Omicron variants (BA.2, BA.1, BA.3, BA.5, BA.4) (Figure 5). These results demonstrate the significance of our proteomics platform in evaluating the broad protective activity of COVID-19 vaccines, which can guide the development of COVID-19 vaccines.

It is important to acknowledge some limitations of our study. First, the *in vitro* detection of NAbs may not represent viral neutralization *in vivo*, although previously reported evidence has shown a good correlation between NAbs detected *in vitro* and *vivo*[5-8]. Second, the relationship between the inhibition levels obtained with the SARS-CoV-2 bNAb assay and the SARS-CoV-2 infection remains unclear. Third, the number of clinical samples employed in this study was limited, and the assay should be executed in a larger cohort to determine the NAb levels induced by different vaccines and infection with SARS-CoV-2 variants. Finally, the SARS-CoV-2 wild-type was not

medRxiv preprint doi: https://doi.org/10.1101/2023.08.07.23293304; this version posted May 10, 2024. The copyright holder for this preprint (which was not certified by peer review) is the author/funder, who has granted medRxiv a license to display the preprint in perpetuity. It is made available under a CC-BY-NC-ND 4.0 International license .

employed due to the unavailability of this protein during executing experiments. Instead, we employed the D614G variant, which shares high homology with the wild type. Previous studies have demonstrated comparable neutralization potency between the D614G variant and the wild type[29]. Additionally, the D614G substitution does not significantly alter SARS-CoV-2 morphology and binding to the ACE2 receptor[30].

Conclusion

We have successfully developed and validated a high-throughput proteomics platform, enabling the comprehensive evaluation of NAbs against a wide range of SARS-CoV-2 variants. This platform offers an efficient, sensitive, and cost-effective approach for detecting broad NAbs within the population, providing an opportunity to guide the design and evaluation of vaccines with enhanced protective efficacy against evolving SARS-CoV-2 strains. Overall, our work contributes to the ongoing efforts in combating the COVID-19 pandemic and advancing our understanding of immune responses to SARS-CoV-2.

References

1. The L. The COVID-19 pandemic in 2023: far from over. *Lancet*. 2023;401(10371):79.
2. Khoury DS, Docken SS, Subbarao K, et al. Predicting the efficacy of variant-modified COVID-19 vaccine boosters. *Nat Med*. 2023;29(3):574-578.
3. Ma Y, Deng J, Liu Q, et al. Long-Term Consequences of Asymptomatic SARS-CoV-2 Infection: A Systematic Review and Meta-Analysis. *Int J Environ Res Public Health*. 2023;20(2).

medRxiv preprint doi: https://doi.org/10.1101/2023.08.07.23293304; this version posted May 10, 2024. The copyright holder for this preprint (which was not certified by peer review) is the author/funder, who has granted medRxiv a license to display the preprint in perpetuity. It is made available under a CC-BY-NC-ND 4.0 International license .

4. Thaweethai T, Jolley SE, Karlson EW, et al. Development of a Definition of Postacute Sequelae of SARS-CoV-2 Infection. *JAMA.* 2023.

5. Nie J, Li Q, Wu J, et al. Quantification of SARS-CoV-2 neutralizing antibody by a pseudotyped virus-based assay. *Nat Protoc.* 2020;15(11):3699-3715.

6. Tan CW, Chia WN, Qin X, et al. A SARS-CoV-2 surrogate virus neutralization test based on antibody-mediated blockage of ACE2-spike protein-protein interaction. *Nat Biotechnol.* 2020;38(9):1073-1078.

7. Fenwick C, Turelli P, Pellaton C, et al. A high-throughput cell- and virus-free assay shows reduced neutralization of SARS-CoV-2 variants by COVID-19 convalescent plasma. *Sci Transl Med.* 2021;13(605).

8. Lynch KL, Zhou S, Kaul R, et al. Evaluation of Neutralizing Antibodies against SARS-CoV-2 Variants after Infection and Vaccination Using a Multiplexed Surrogate Virus Neutralization Test. *Clin Chem.* 2022;68(5):702-712.

9. Perkmann T, Mucher P, Osze D, et al. Comparison of five Anti-SARS-CoV-2 antibody assays across three doses of BNT162b2 reveals insufficient standardization of SARS-CoV-2 serology. *J Clin Virol.* 2023;158:105345.

10. Bal A, Pozzetto B, Trabaud MA, et al. Evaluation of High-Throughput SARS-CoV-2 Serological Assays in a Longitudinal Cohort of Patients with Mild COVID-19: Clinical Sensitivity, Specificity, and Association with Virus Neutralization Test. *Clin Chem.* 2021;67(5):742-752.

11. Grant R, Sacks J, Abraham P, et al. When to update COVID-19 vaccine composition. *Nature Medicine* 2023(29):776–780.

12. Chao Z, Han Y, Jiao Z, et al. Prism Design for Spectral Flow Cytometry. *Micromachines (Basel).* 2023;14(2).

13. Yu X, Hartmann M, Wang Q, et al. microFBI: a microfluidic bead-based immunoassay for multiplexed detection of proteins from a microL sample volume. *PLoS One.* 2010;5(10).

14. Wang Q, Guo Y, Iketani S, et al. Antibody evasion by SARS-CoV-2 Omicron subvariants BA.2.12.1, BA.4 and BA.5. *Nature.* 2022;608(7923):603-608.

15. Mahalingam G, Arjunan P, Periyasami Y, et al. Correlating the differences in the receptor binding domain of SARS-CoV-2 spike variants on their interactions with human ACE2 receptor. *Sci Rep.* 2023;13(1):8743.

16. Gorbalenya AE, Baker SC, Baric RS, et al. The species Severe acute respiratory syndrome-related coronavirus: classifying 2019-nCoV and naming it SARS-CoV-2. *Nature Microbiology.* 2020;5(4):536-544.

17. Zhan H, Gao H, Liu Y, et al. Booster shot of inactivated SARS-CoV-2 vaccine induces potent immune responses in people living with HIV. *J Med Virol.* 2023;95(1):e28428.

18. Marien J, Michiels J, Heyndrickx L, et al. Evaluation of a surrogate virus neutralization test for high-throughput serosurveillance of SARS-CoV-2. *J Virol Methods.* 2021;297:114228.

19. Chen Y, Zhao X, Zhou H, et al. Broadly neutralizing antibodies to SARS-CoV-2 and other human coronaviruses. *Nat Rev Immunol.* 2023;23(3):189-199.

20. Liang T, Cheng M, Teng F, et al. Proteome-wide epitope mapping identifies a

medRxiv preprint doi: https://doi.org/10.1101/2023.08.07.23293304; this version posted May 10, 2024. The copyright holder for this preprint (which was not certified by peer review) is the author/funder, who has granted medRxiv a license to display the preprint in perpetuity. It is made available under a CC-BY-NC-ND 4.0 International license .

resource of antibodies for SARS-CoV-2 detection and neutralization. *Signal Transduct Target Ther.* 2021;6(1):166.

21. Zhao X, Zhang R, Qiao S, et al. Omicron SARS-CoV-2 Neutralization from Inactivated and ZF2001 Vaccines. *N Engl J Med.* 2022;387(3):277-280.

22. Zhang J, Teng F, Zhang X, et al. Down-regulation of SARS-CoV-2 neutralizing antibodies in vaccinated smokers. *MedComm (2020).* 2022;3(3):e166.

23. Faraone JN, Qu P, Goodarzi N, et al. Immune evasion and membrane fusion of SARS-CoV-2 XBB subvariants EG.5.1 and XBB.2.3. *Emerging Microbes & Infections.* 2023;12(2).

24. Antinori A, Bausch-Jurken M. The Burden of COVID-19 in the Immunocompromised Patient: Implications for Vaccination and Needs for the Future. *The Journal of Infectious Diseases.* 2023;228(Supplement_1):S4-S12.

25. Lotfi H, Mazar MG, Ei NMH, et al. Vaccination is the most effective and best way to avoid the disease of COVID-19. *Immunity, Inflammation and Disease.* 2023;11(8).

26. Yin W, Xu Y, Xu P, et al. Structures of the Omicron spike trimer with ACE2 and an anti-Omicron antibody. *Science.* 2022;375(6584):1048-1053.

27. Ma W, Fu H, Jian F, et al. Immune evasion and ACE2 binding affinity contribute to SARS-CoV-2 evolution. *Nat Ecol Evol.* 2023.

28. Markov PV, Katzourakis A, Stilianakis NI. Antigenic evolution will lead to new SARS-CoV-2 variants with unpredictable severity. *Nat Rev Microbiol.* 2022;20(5):251-252.

29. Yurkovetskiy L, Wang X, Pascal KE, et al. Structural and Functional Analysis of the D614G SARS-CoV-2 Spike Protein Variant. *Cell.* 2020;183(3):739-751 e738.

30. Hou YJ, Chiba S, Halfmann P, et al. SARS-CoV-2 D614G variant exhibits efficient replication ex vivo and transmission in vivo. *Science*. 2020;370(6523):1464-1468.

31. Zhang X, Zheng M, Wang H, et al. Inhibitor screening using microarray identifies the high capacity of neutralizing antibodies to Spike variants in SARS-CoV-2 infection and vaccination. *Theranostics.* 2022;12(6):2519-2534.

32. Yang L, Yu Y, Ma C, et al. Development of RBC Membrane Antigen Arrays for Validating Blood Grouping Reagents. *J Proteome Res.* 2018;17(9):3237-3245.

33. Salazar-García M, Acosta-Contreras S, Rodríguez-Martínez G, et al. Pseudotyped Vesicular Stomatitis Virus-Severe Acute Respiratory Syndrome-Coronavirus-2 Spike for the Study of Variants, Vaccines, and Therapeutics Against Coronavirus Disease 2019. *Frontiers in Microbiology.* 2022;12.

34. Nie J, Li Q, Wu J, et al. Establishment and validation of a pseudovirus neutralization assay for SARS-CoV-2. *Emerging Microbes & Infections.* 2020;9(1):680-686.

35. Chen G-L, Li X-F, Dai X-H, et al. Safety and immunogenicity of the SARS-CoV-2 ARCoV mRNA vaccine in Chinese adults: a randomised, double-blind, placebo-controlled, phase 1 trial. *The Lancet Microbe.* 2022;3(3):e193-e202.

36. Robin X, Turck N, Hainard A, et al. pROC: an open-source package for R and S+ to analyze and compare ROC curves. *BMC Bioinformatics.* 2011;12:77.

medRxiv preprint doi: https://doi.org/10.1101/2023.08.07.23293304; this version posted May 10, 2024. The copyright holder for this preprint (which was not certified by peer review) is the author/funder, who has granted medRxiv a license to display the preprint in perpetuity. It is made available under a CC-BY-NC-ND 4.0 International license .

Contributions

X.Z. and D.H. executed the experiments; M.L., X. Z., X.Z., X.X., T. L., and Y. Z. performed the data analysis; H.L. and Y.W. provided the clinical samples. X.Y., Y. L., B.W. and X.Z. wrote and revised the paper.

Acknowledgment

This work was supported by the Beijing Municipal Natural Science Foundation (M23010 and L234034), National Key R&D Program of China(2022YFE0210400, 2021YFA1301604, 2020YFE0202200), State Key Laboratory of Proteomics (SKLP-O202007), Academic leader of high-level public health technical personnel construction project of Beijing Municipal Health Commission (2022-2-014), Guangdong Province Science and Technology Planning Project (2020B1111100006), Innovation Team and Talents Cultivation Program of National Administration of Traditional Chinese Medicine. (No: ZYYCXTD-C-202204). We would like to thank the bioinformatics platform of the National Center for Protein Sciences (Beijing) for their support in the data analysis of this project. We also thank Dr. Brianne Petritis for her critical review and editing of this manuscript.

Declaration of Interest Statement

The authors have declared no conflict of interest.

medRxiv preprint doi: https://doi.org/10.1101/2023.08.07.23293304; this version posted May 10, 2024. The copyright holder for this preprint (which was not certified by peer review) is the author/funder, who has granted medRxiv a license to display the preprint in perpetuity. It is made available under a CC-BY-NC-ND 4.0 International license .

Supplementary materials

This article contains Supplementary Figure 1-4 and Supplementary Table1-7.

Tables

Table 1. Clinical serum samples employed in this study

		3rd dose vaccination cohort (n=56)
Gender		
	Male	16(28.6%)
	Female	40(71.4%)
Age (years)		
	Range	21-70
	≤50	50(89.3%)
	>50	6(10.7%)
Vaccination type		
Recombinant RBD-subunit vaccine (ZF2001)		38(83.9%)
Inactivated vaccine (Sinovac-CoronaVac)		18(16.1%)
Days of serum collection after 3rd dose vaccination		28

Figure legends

Figure 1. Schematic illustration of the high throughput SARS-CoV-2 bNAb assay. (A) Workflow of the SARS-CoV-2 bNAb assay. The Spike-ACE2 interaction is a direct binding reaction between Spike trimer proteins and biotinylated ACE2. Upon the addition of the

medRxiv preprint doi: https://doi.org/10.1101/2023.08.07.23293304; this version posted May 10, 2024. The copyright holder for this preprint (which was not certified by peer review) is the author/funder, who has granted medRxiv a license to display the preprint in perpetuity. It is made available under a CC-BY-NC-ND 4.0 International license .

NAbs, the beads coupled with SARS-CoV-2 variants Spike trimer proteins are incubated with NAbs. The NAbs with neutralizing activity will block the Spike interaction with biotinylated ACE2 and SA-PE. The signal intensities of the Spike trimer-ACE2 interaction are inversely proportional to the level of NAbs. During the NAbs detection process, all coupled beads were mixed together and incubated with samples containing NAbs. The NAbs bound to the Spike trimer proteins, preventing their interaction with the biotinylated ACE2 receptors, which were coupled to streptavidin-phycoerythrin (SA-PE). (B) Dose relationship curve of Spike-ACE2 interactions using Wellgrow and Luminex platforms. MFI = mean fluorescence intensity. (C) A comparison of the sensitivity to detect Spike-ACE2 interactions with the Wellgrow and Luminex platforms.

Figure 2. Spike trimer-ACE2 interactions across different SARS-CoV-2 variants and ACE2 concentrations. (A) Dose relationship curve of the interactions between ACE2 and six SARS-CoV-2 non-Omicron variants and five Omicron variants The x-axis represents the concentrations of the host ACE2 receptor. The y-axis represents the median of fluorescent signal intensity (MFI) of the SARS-CoV-2 Spike trimer-ACE2 interaction. N = nucleocapsid protein, which was used as a negative control. (B) Distribution of the NAb

medRxiv preprint doi: https://doi.org/10.1101/2023.08.07.23293304; this version posted May 10, 2024. The copyright holder for this preprint (which was not certified by peer review) is the author/funder, who has granted medRxiv a license to display the preprint in perpetuity. It is made available under a CC-BY-NC-ND 4.0 International license .

resistance to SARS-CoV-2 variants. The x-axis represents the SARS-CoV-2 variants. The y-axis represents the EC50 calculated from SARS-CoV-2 variant Spike-ACE2 interactions. The corresponding values on the Y-axis are Omicron BA.1 (0.2913 µg/mL), Beta (0.2913 µg/mL), Delta (0.3415 µg/mL), Omicron BA.4 (0.3592 µg/mL), Gamma (0.3833 µg/mL), Alpha (0.394 µg/mL), Kappa (0.3983 µg/mL), Omicron BA. 2 (0.4307µg/mL), Omicron BA. 5(0.4593 µg/mL), D614G (0.5279 µg/mL), and Omicron BA.3 (1.283 µg/mL), respectively.

Figure 3. Comparison of SARS-CoV-2 bNAb assay to ELISA , cPass sVNT, pseudovirus-based neutralization and live virus based neutralization assays. (A) Correlation analysis of serological IgG detection between the SARS-CoV-2 bNAb assay and an ELISA-based IgG serology. (B) Correlation analysis of NAb detection using the SARS-CoV-2 bNAb assay and the FDA-approved cPass sVNT test. The concordance of NAb detection using the ELISA and sVNT assays was calculated as the positive and negative percent agreement (PPA and NPA, respectively). The blue and red dots represent positive (neutralizing activity) and negative (non-neutralizing) cases as determined by the comparative analysis, respectively. (C) Correlation analysis of D614G NAbs inhibition rate (%) from the SARS-CoV-2 bNAb assay with WT NAb titers from pseudovirus-based

medRxiv preprint doi: https://doi.org/10.1101/2023.08.07.23293304; this version posted May 10, 2024. The copyright holder for this preprint (which was not certified by peer review) is the author/funder, who has granted medRxiv a license to display the preprint in perpetuity. It is made available under a CC-BY-NC-ND 4.0 International license .

neutralization assays. (D) Correlation analysis of BA.1 NAbs inhibition rate (%) from the SARS-CoV-2 bNAb assay with BA.1 NAb titers from pseudovirus-based neutralization assays. (E) Correlation analysis of D614G NAbs inhibition rate (%) from the SARS-CoV-2 bNAb assay with WT NAb titers from live virus based neutralization assays. (F) Correlation analysis of BA.1 NAbs inhibition rate (%) from the SARS-CoV-2 bNAb assay with BA.1 NAb titers from live virus based neutralization assays.

Figure 4. Identification of monoclonal/polyclonal Abs with broad neutralizing capability. (A) Dose relationship curve demonstrating the ability of the NAb to inhibit SARS-CoV-2 variant Spike trimer-ACE2 interactions. The x-axis represents the concentrations of the NAb. The y-axis represents the percent activity (%) of the NAb. N = nucleocapsid protein, which was used as a negative control. (B) Heatmap showing the IC50 of NAbs against different SARS-CoV-2 variants. The detail of monoclonal/polyclonal Abs are provided in Table S5.

Figure 5. Detection of serum NAbs in vaccinated individuals. (A) Boxplot showing the distribution of inhibition rate (%) of serum NAbs against SARS-CoV-2 variants in 56 vaccinated individuals. (B) Comparison of NAbs produced between groups receiving the

medRxiv preprint doi: https://doi.org/10.1101/2023.08.07.23293304; this version posted May 10, 2024. The copyright holder for this preprint (which was not certified by peer review) is the author/funder, who has granted medRxiv a license to display the preprint in perpetuity. It is made available under a CC-BY-NC-ND 4.0 International license .

inactivated vaccine (Sinovac-CoronaVac) or recombinant subunit vaccine (ZF2001). The significance was performed using the Student's *t*-test (p-value < 0.01). **, ***, and **** represent a p-value less than 0.01, 0.001, and 0.0001, respectively.

Materials and methods

Collection of clinical samples

Clinical serum samples were collected from Beijing Ditan Hospital 28 days after the third dose of the COVID-19 vaccine (Table 1). Whole blood was collected in a vacutainer tube, and the serum was obtained via centrifugation at 4,000 × g at room temperature for 10 minutes. The serum was then transferred to a clean tube and stored at -80 °C until use. This study was approved by the Ethics Committee of Beijing Ditan Hospital (No.2021-010-01), and an exemption of informed consent was obtained before sera collection[31].

Preparation of SARS-CoV-2 bNAb reagents

The SARS-CoV-2 bNAb assay was developed in ProteomicsEra Medical Co., Ltd (Beijing, China). Briefly, 3 μg SARS-CoV-2 Spike trimer proteins (Sino Biological., Novoprotein and ACROBiosystems; China) (Table S1) were coupled to 1×10^6 magnetic-fluorescent beads (Wellgrow Technology Co., Ltd.) as previously described[32]. First, 12

medRxiv preprint doi: https://doi.org/10.1101/2023.08.07.23293304; this version posted May 10, 2024. The copyright holder for this preprint (which was not certified by peer review) is the author/funder, who has granted medRxiv a license to display the preprint in perpetuity. It is made available under a CC-BY-NC-ND 4.0 International license .

differently encoded magnetic-fluorescent beads, numbered 102-108 and 201-205 (Table S2), were chosen. Then 125 μL containing 1×10^6 beads were washed with 100 μL ddH2O and activated with 80 μL of "activation buffer" (50 mM 2-(N-morpholino) ethanesulfonic acid (MES) pH 5.0) (Sigma-Aldrich, St. Louis, MO). Then the activated beads were mixed with 10 μL of 50 mg/mL sulfo-N-hydroxysuccinimide (NHS) (Thermo Scientific, USA) and 10 μL of 50 mg/mL 1-Ethyl-3-[3-dimethylaminopropyl]-carbodiimide hydrochloride (EDC) (Solarbio, Beijing, China). After incubation for 20 min at room temperature with gentle mixing, the beads were washed twice with 250 μL "coupling buffer" (50 mM MES pH 5.0) and resuspended in 200 μL coupling buffer. Then 3 μg of Spike trimer proteins were added to the bead solution and incubated for 2 h at room temperature. After washing, the beads underwent blocking with "blocking buffer" (PBST-B, PBS pH 7.4, 0.05% Tween-20, 1% BSA), and the coupled beads were subsequently stored at 2-8 °C in "storage buffer" (PBST-BN, PBS pH 7.4, 0.05% Tween-20, 0.1% BSA, 0.05% NaN3).

Detection of Spike-ACE2 interactions using SARS-CoV-2 bNAb assay

First, a 50 μL mixed solution containing 12 different SARS-CoV-2 Spike trimer protein-coupled beads (2500 beads per type) (Table S3) was

medRxiv preprint doi: https://doi.org/10.1101/2023.08.07.23293304; this version posted May 10, 2024. The copyright holder for this preprint (which was not certified by peer review) is the author/funder, who has granted medRxiv a license to display the preprint in perpetuity. It is made available under a CC-BY-NC-ND 4.0 International license .

added to each well of a 96-well plate, followed by 50 μL of different concentrations (0, 0.014, 0.041, 0.123, 0.370, 1.111, 3.333, 10 μg/mL) of biotinylated ACE2 (Sino Biological). After incubation for 1 h at room temperature on a shaker, the beads were magnetically separated using a magnetic separator (Wellgrow Technology Co., Ltd.) and washed three times with 100 μL PBST-B (PBS pH7.4，0.05% Tween-20, 0.1% BSA). After washing, the Spike-ACE2 interaction was detected using 50 μL SA-PE (Thermo Scientific, USA) (2 μg/mL) for 30 minutes at room temperature. Finally, after washing with PBST-B twice, the beads were resuspended in a 200 μL PBST-B solution. The fluorescent signal was then detected at 200 beads/region using the EasyCell flow cytometry (Wellgrow Technology Co., Ltd.) with excitation wavelengths of 532 nm and 635 nm.

Detection of monoclonal/polyclonal NAbs using the SARS-CoV-2 bNAb assay

To detect monoclonal/polyclonal NAbs, a 50 μL mixed solution containing 7 different SARS-CoV-2 Spike trimer protein-coupled beads (2500 beads per type) (Table S4) was added to each well of a 96-well plate. Following that, 50 μL of each antibody solution at different concentrations (0, 0.014, 0.041, 0.123, 0.370, 1.111, 3.333, 10 μg/mL) for anti-Spike antibodies (#26, #20, #21, #22, #23, #73) (Table S5) was

medRxiv preprint doi: https://doi.org/10.1101/2023.08.07.23293304; this version posted May 10, 2024. The copyright holder for this preprint (which was not certified by peer review) is the author/funder, who has granted medRxiv a license to display the preprint in perpetuity. It is made available under a CC-BY-NC-ND 4.0 International license .

added to individual wells of a 96-well plate. After incubation for 2 h at room temperature on a shaker, the beads were washed with PBST-B three times, then the beads were incubated with 50 μL biotinylated ACE2 (0.5 μg/mL) for 1 hour at room temperature. After washing, the binding of ACE2 to Spike trimer proteins were detected using 50 μL SA-PE (2 μg/mL) for 30 minutes at room temperature. Finally, after washing with PBST-B twice, the beads were resuspended in a 200 μL PBST-B solution. The fluorescent signal was then detected at 200 beads/region using the EasyCell flow cytometry (Wellgrow Technology Co., Ltd.) with excitation wavelengths of 532 nm and 635 nm.

Detection of Serum NAbs using SARS-CoV-2 bNAb assay.

First, a 50 μL mixed solution containing 12 different SARS-CoV-2 Spike trimer protein-coupled beads (2500 beads per type) (Table S2) was added to each well of a 96-well plate, followed by 50 μL of the serum samples which were diluted to 1:20 with PBST-B. After incubation for 2 h at room temperature on a shaker, the beads were washed with PBST-B three times. Then the beads were incubated with 50 μL biotinylated ACE2 (0.5 μg/mL) for 1 hour at room temperature. After washing, the binding of ACE2 to Spike trimer proteins were detected using 50 μL SA-PE (2 μg/mL) and incubated the mixture for 30 minutes at room temperature. Finally, after washing with PBST-B twice, the

medRxiv preprint doi: https://doi.org/10.1101/2023.08.07.23293304; this version posted May 10, 2024. The copyright holder for this preprint (which was not certified by peer review) is the author/funder, who has granted medRxiv a license to display the preprint in perpetuity. It is made available under a CC-BY-NC-ND 4.0 International license .

beads were resuspended in a 200 μL PBST-B solution. The fluorescent signal was then detected at 200 beads/region using the EasyCell flow cytometry (Wellgrow Technology Co., Ltd.) with excitation wavelengths of 532 nm and 635 nm.

Detection of Serum NAbs using the anti-Spike RBD IgG antibodies obtained by the ELISA.

The assay was conducted as described previously[17]. A capture sandwich ELISA detection kit (PROPRIUM, Hangzhou, China) was used to detect SARS-CoV-2 antibodies against the Spike protein RBD. The SARS-CoV-2 Spike RBD protein was pre-coated onto the solid phase, allowing it to form an antigen-antibody complex with IgG anti-RBD antibodies from 100 μL of diluted serum samples (1:30 dilution ratio) or standards. After washing, HRP-conjugated anti-human IgG was added to form an antigen-antibody-HRP complex. The substrate solution TMB was then introduced, and the resulting color intensity was proportional to the level of SARS-CoV-2-neutralizing antibodies. The optical density (OD) at 450 nm was measured, and a threshold of 10 BAU/ml was used to determine sero-positive and negative samples for anti-Spike RBD IgG.

Detection of Serum NAbs using cPass™ sVNT Kit.

medRxiv preprint doi: https://doi.org/10.1101/2023.08.07.23293304; this version posted May 10, 2024. The copyright holder for this preprint (which was not certified by peer review) is the author/funder, who has granted medRxiv a license to display the preprint in perpetuity. It is made available under a CC-BY-NC-ND 4.0 International license .

The assay was conducted as described previously[17]. Using competitive ELISA, the SARS-CoV-2 Surrogate Virus Neutralization Test (sVNT) assay (Genscript, Nanjing, China) identified neutralizing antibodies present in the bloodstream that obstruct the interaction between the viral Spike glycoprotein receptor-binding domain (RBD) and human ACE2. Following the manufacturer's instructions, diluted serum samples (1:10 dilution ratio) and controls were pre-incubated at 37□ for 15 minutes to allow binding of neutralizing antibodies (NAb) and HRP-RBD (antigen derived from SARS-CoV-2 variant D614G), using a 1:1 volume ratio. Subsequently, the mixture was transferred to a capture plate, pre-coated with hACE2 protein, where NAb-unbound HRP-RBD was captured on the plate, while NAb-bound HRP-RBD remained in the supernatant and was washed away. Next, 100 μL of TMB and 50 μL of stop solution were added, and the plate was read at 450 nm. The sample's absorbance was inversely correlated with the titers of anti-SARS-CoV-2-neutralizing antibodies. To ensure result validity, the OD450 values of positive controls (> 1.0) and negative controls (< 0.3) had to fall within specific ranges. An inhibition rate of ≥ 30% was considered positive for SARS-CoV-2-neutralizing antibody determination. The inhibition rate was calculated as follows: Inhibition□=□(1 - OD value of sample/OD value of negative control)□×□100%.

medRxiv preprint doi: https://doi.org/10.1101/2023.08.07.23293304; this version posted May 10, 2024. The copyright holder for this preprint (which was not certified by peer review) is the author/funder, who has granted medRxiv a license to display the preprint in perpetuity. It is made available under a CC-BY-NC-ND 4.0 International license .

Pseudovirus-based neutralization assay.

The SARS-CoV-2 pseudovirus was prepared using the VSV-ΔG system in which the glycoprotein (G) gene was replaced with the firefly luciferase (Fluc) reporter gene [33,34]. The S protein was overexpressed and displayed on the VSV pseudovirus. Following S-ACE2 interaction, the pseudovirus entered the host cell where the Fluc gene was transcribed and translated. The addition of luciferase substrate resulted in luminescence where the amount of luminescence is proportional to the level of pseudoviral entry. The preparation process of SARS-CoV-2 pseudovirus begins with the cloning of the S gene encoding the S protein of the virus. Subsequently, this gene is inserted into a modified VSV backbone, replacing the original G gene. The resulting construct, containing the S protein gene in lieu of the G gene and complemented by the Fluc reporter gene, forms the foundation of the pseudovirus. The pseudovirus equipped with the S protein can interact with the ACE2 receptor on the surface of host cells, thereby facilitating the entry of the pseudovirus into the cells. Once inside the cells, the Fluc gene will be transcribed and translated to produce luciferase.

The assay was conducted following previously described methods[20,35]. Huh7 cells were seeded at a concentration of 2×10^4

medRxiv preprint doi: https://doi.org/10.1101/2023.08.07.23293304; this version posted May 10, 2024. The copyright holder for this preprint (which was not certified by peer review) is the author/funder, who has granted medRxiv a license to display the preprint in perpetuity. It is made available under a CC-BY-NC-ND 4.0 International license .

cells per well in 96-well plates and incubated until reaching 90-100% confluency, typically around 24 hours. Serum samples, subjected to serial 3-fold dilutions commencing at 1:10, were then incubated with 650 TCID50 of the pseudovirus for a precisely controlled duration of 1 hour at 37 °C. Dulbecco's modified eagle medium (DMEM) served as the negative control. As a crucial negative control, Dulbecco's Modified Eagle Medium (DMEM) was employed. Following the incubation period, the supernatant was carefully aspirated, making way for the addition of luciferase substrate to each well. A subsequent 2-minute incubation in darkness at room temperature facilitated optimal enzymatic reactions. Luciferase activity, indicative of neutralizing antibody presence, was quantified using the GloMax® 9633 Microplate Luminometer (Promega, Madison, USA).

Live virus based neutralization assay.

The assay was conducted as described previously[35]. To assess the SARS-CoV-2-specific NAb titer in serum, we employed a cytopathic effect (CPE)-based microneutralization assay, utilizing the SARS-CoV-2 virus strain BetaCoV/Beijing/IME-BJ01/2020 (Accession No. GWHACAX01000000) and Vero cells (ATCC, CCL81). Serum samples underwent heat inactivation for 30 minutes at 56 °C and were subsequently two-fold serially diluted (ranging from 1:4 to 1:2048)

medRxiv preprint doi: https://doi.org/10.1101/2023.08.07.23293304; this version posted May 10, 2024. The copyright holder for this preprint (which was not certified by peer review) is the author/funder, who has granted medRxiv a license to display the preprint in perpetuity. It is made available under a CC-BY-NC-ND 4.0 International license .

using Dulbecco's Modified Eagle Medium (DMEM) from Thermo Fisher Scientific. These dilutions were then mixed with an equivalent volume of the virus solution to achieve a 50% tissue culture infectious dose (TCID50) of 100 in each well.

The serum-virus mixtures were incubated for 1 hour at 37 °C to allow for sufficient neutralization reactions to occur. Following incubation, the mixtures were gently added to 96-well plates containing semi-confluent Vero cells with a density exceeding 80%. The plates were then incubated for a further 3 days at 37 °C to allow for the development of cytopathic effects (CPEs) on the Vero cells. Using an inverted microscope, the CPEs on the Vero cells were carefully observed and recorded. The neutralizing titer was determined as the reciprocal of the highest sample dilution that successfully protected at least 50% of the cells from CPE. In cases where no neutralization reaction was observable even at the initial serum dilution of 1:4, an arbitrary titer of 2 (half of the limit of quantification) was assigned.

Data analysis

To compare the inhibition rate (%) of serum NAbs against the D614G variant and other SARS-CoV-2 variants, the raw inhibition rates of different variants were first normalized using minimum-maximum normalization. Statistical analyses were performed using Student's

medRxiv preprint doi: https://doi.org/10.1101/2023.08.07.23293304; this version posted May 10, 2024. The copyright holder for this preprint (which was not certified by peer review) is the author/funder, who has granted medRxiv a license to display the preprint in perpetuity. It is made available under a CC-BY-NC-ND 4.0 International license .

t-test, with a p-value $\leq$ 0.01 considered as statistically significant. Correlations between the SARS-CoV-2 bNAb, ELISA-based serology test, and the cPass sVNT test were determined using Pearson correlation coefficients. Positive and negative percent agreement (PPA, NPA) were performed using the positive and negative judgment results from ELISA-based IgG serology and cPass sVNT tests. Ideal cutoffs for the SARS-CoV-2 bNAb method that maximized PPA and NPA were calculated using the Youden Index, which was implemented in the R package pROC (v 1.18.2) [36]. All data analyses were carried out in R (v4.2.3) under the R studio (v 19.1.3) environment.

Figure 1

medRxiv preprint doi: https://doi.org/10.1101/2023.08.07.23293304; this version posted May 10, 2024. The copyright holder for this preprint (which was not certified by peer review) is the author/funder, who has granted medRxiv a license to display the preprint in perpetuity. It is made available under a CC-BY-NC-ND 4.0 International license .

A

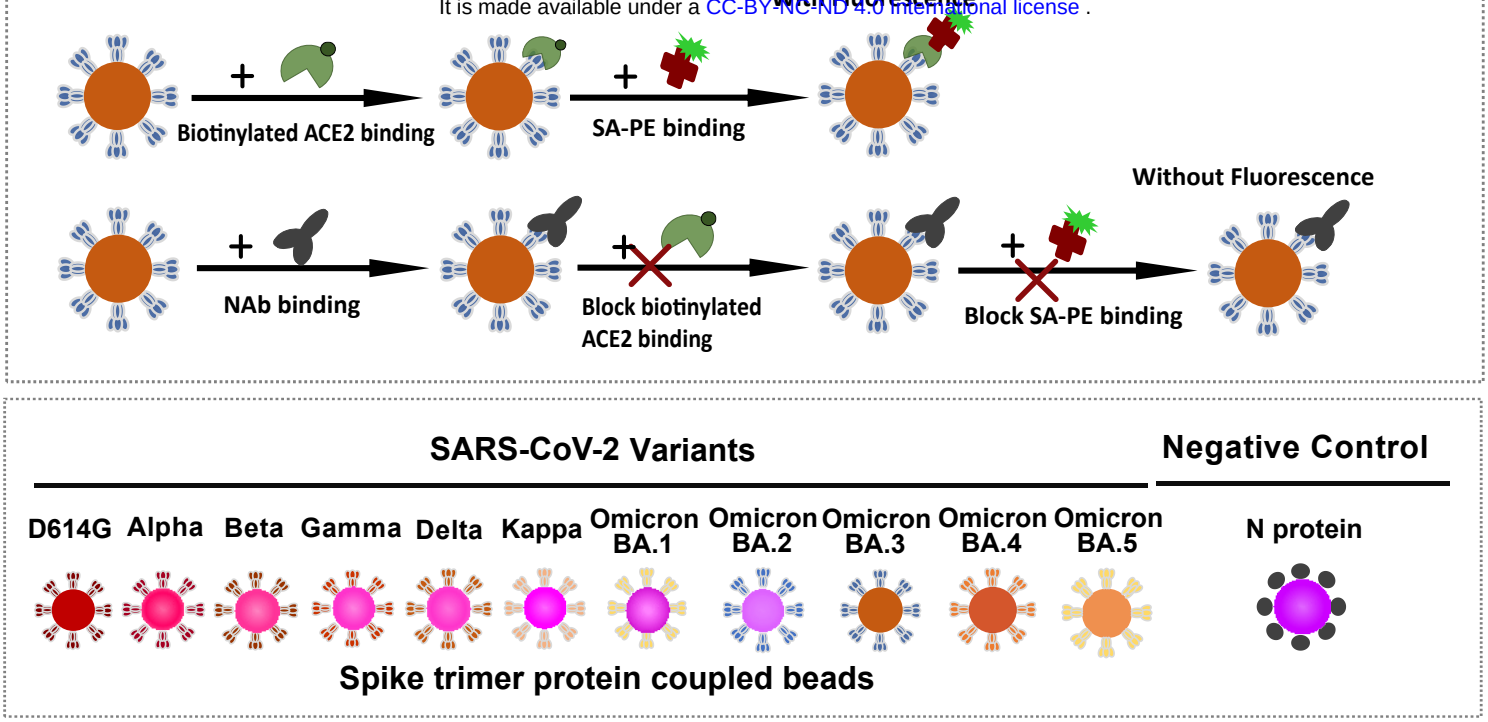

B

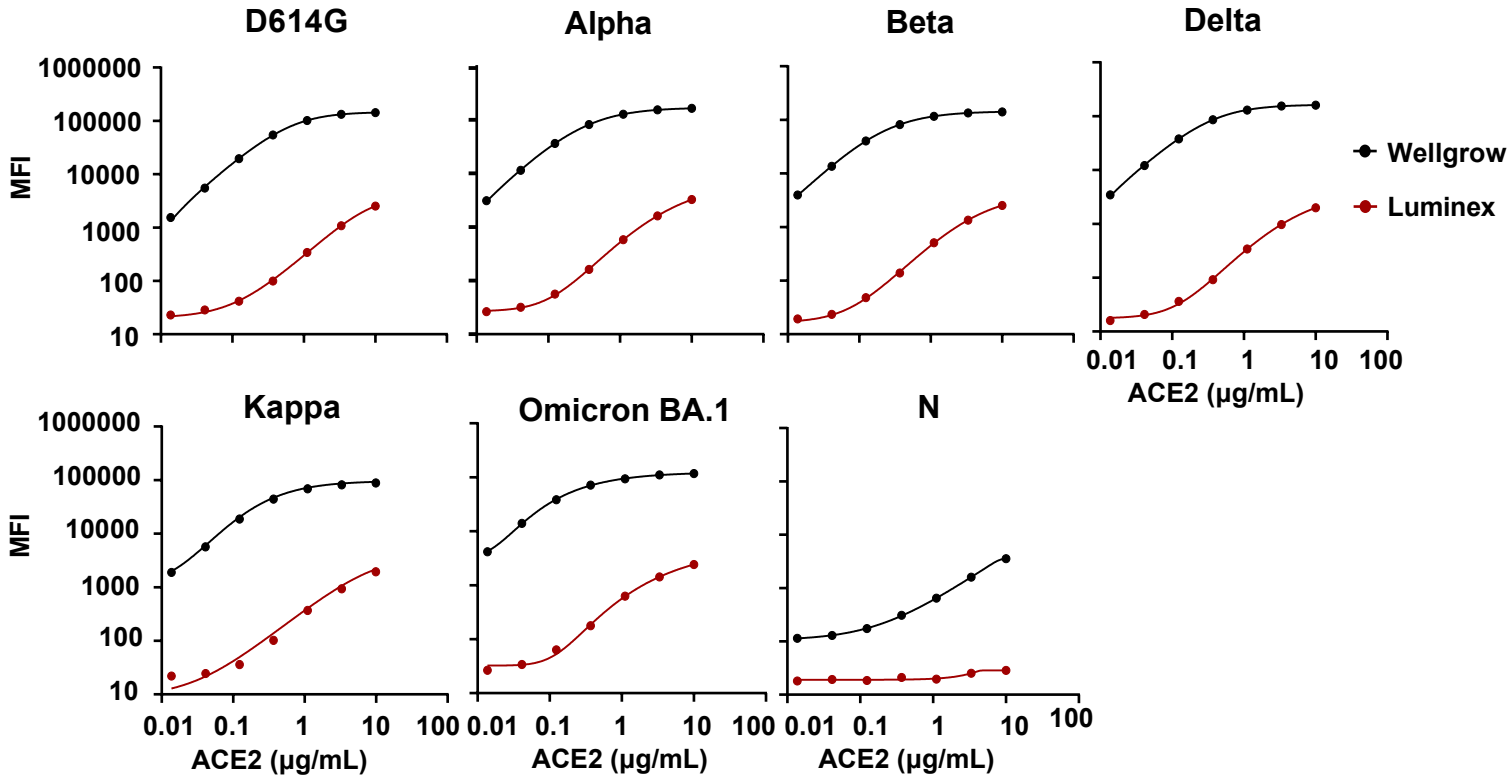

C

LOD [μg/mL]	D614G	Alpha	Beta	Delta	Kappa	Omicron BA.1	Average
Luminex	0.19	0.12	0.16	0.23	0.14	0.12	0.16
Wellgrow	0.006	0.003	0.005	0.003	0.007	0.008	0.005
Fold change [L/W] (×)	31.67	40	32	76.67	20	15	35.89±57.80 [-21.91～93.69]

Figure 2

medRxiv preprint doi: https://doi.org/10.1101/2023.08.07.23293304; this version posted May 10, 2024. The copyright holder for this preprint (which was not certified by peer review) is the author/funder, who has granted medRxiv a license to display the preprint in perpetuity. It is made available under a CC-BY-NC-ND 4.0 International license .

A

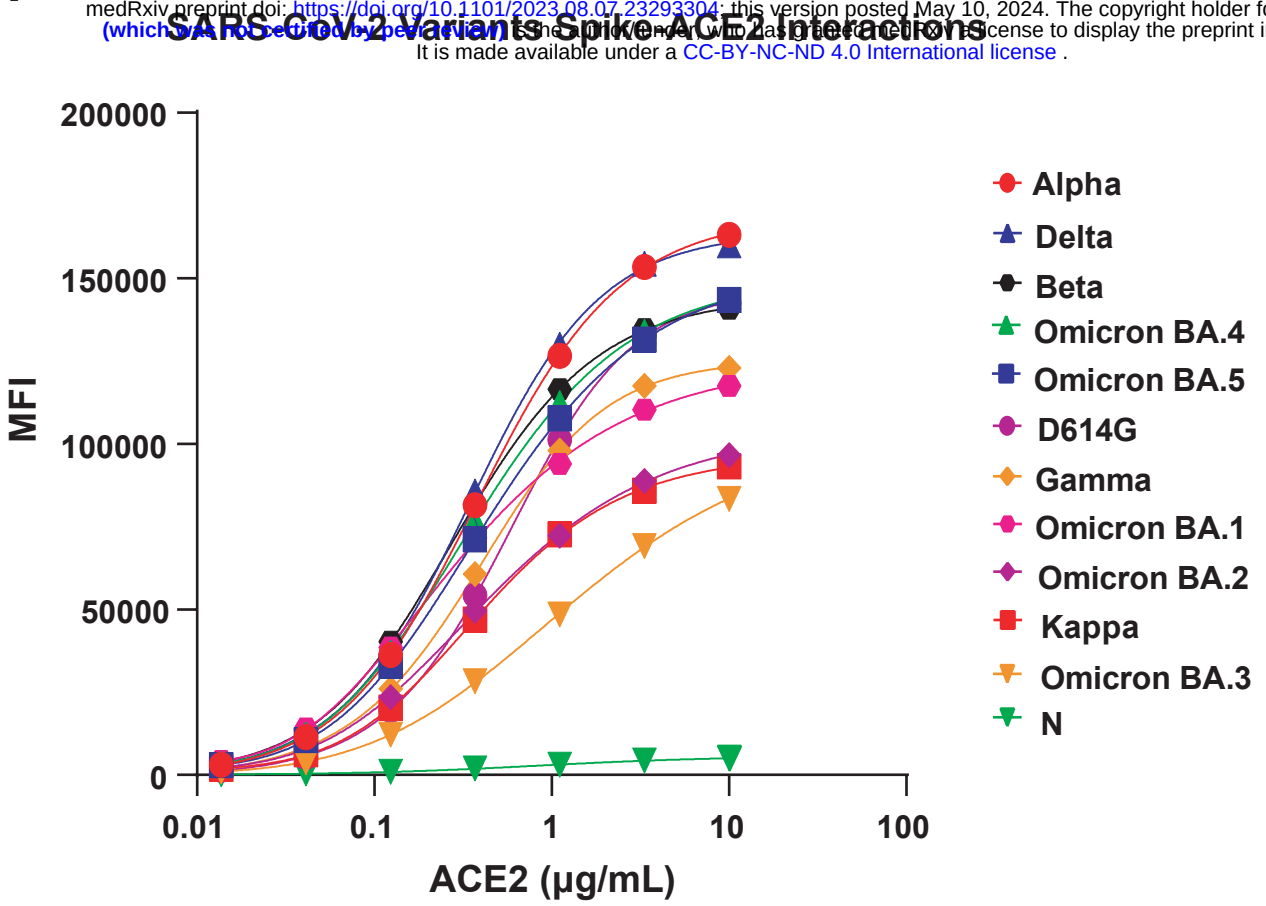

B

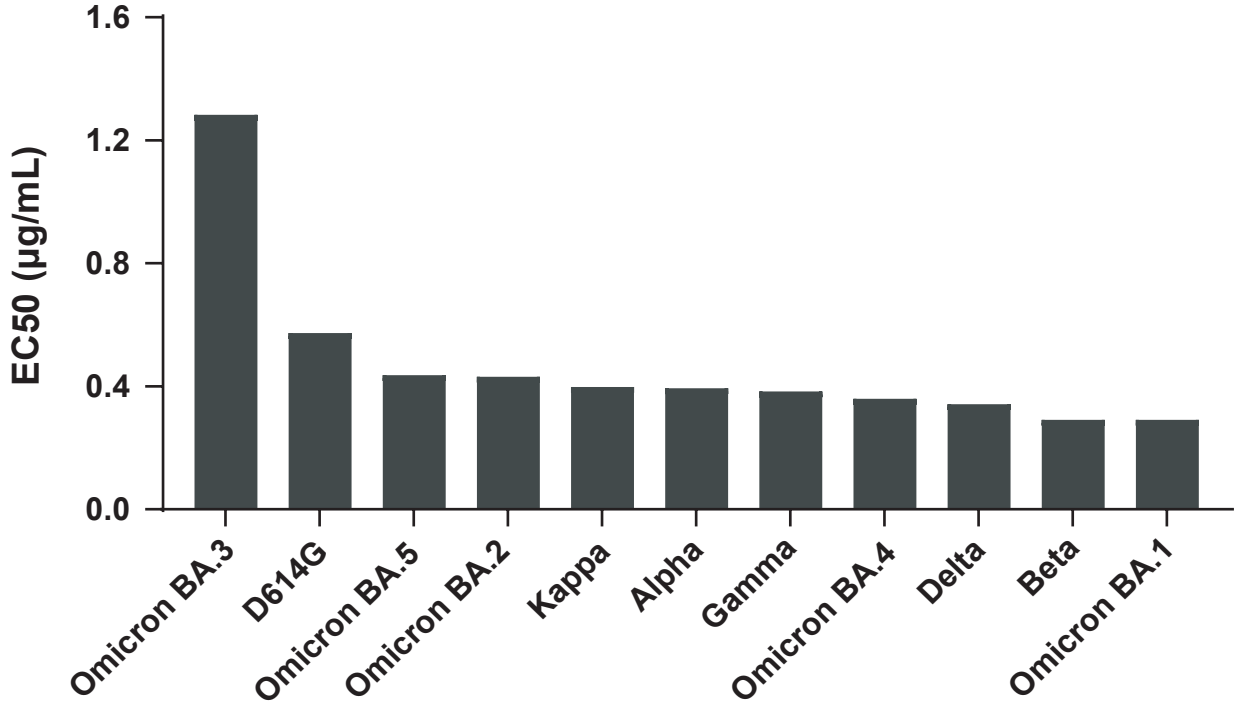

Figure 3

medRxiv preprint doi: https://doi.org/10.1101/2023.08.07.23293304, this version posted May 10, 2024. The copyright holder for this preprint (which was not certified by peer review) is the author/funder, who has granted medRxiv a license to display the preprint in perpetuity. It is made available under a CC-BY-NC-ND 4.0 International license .

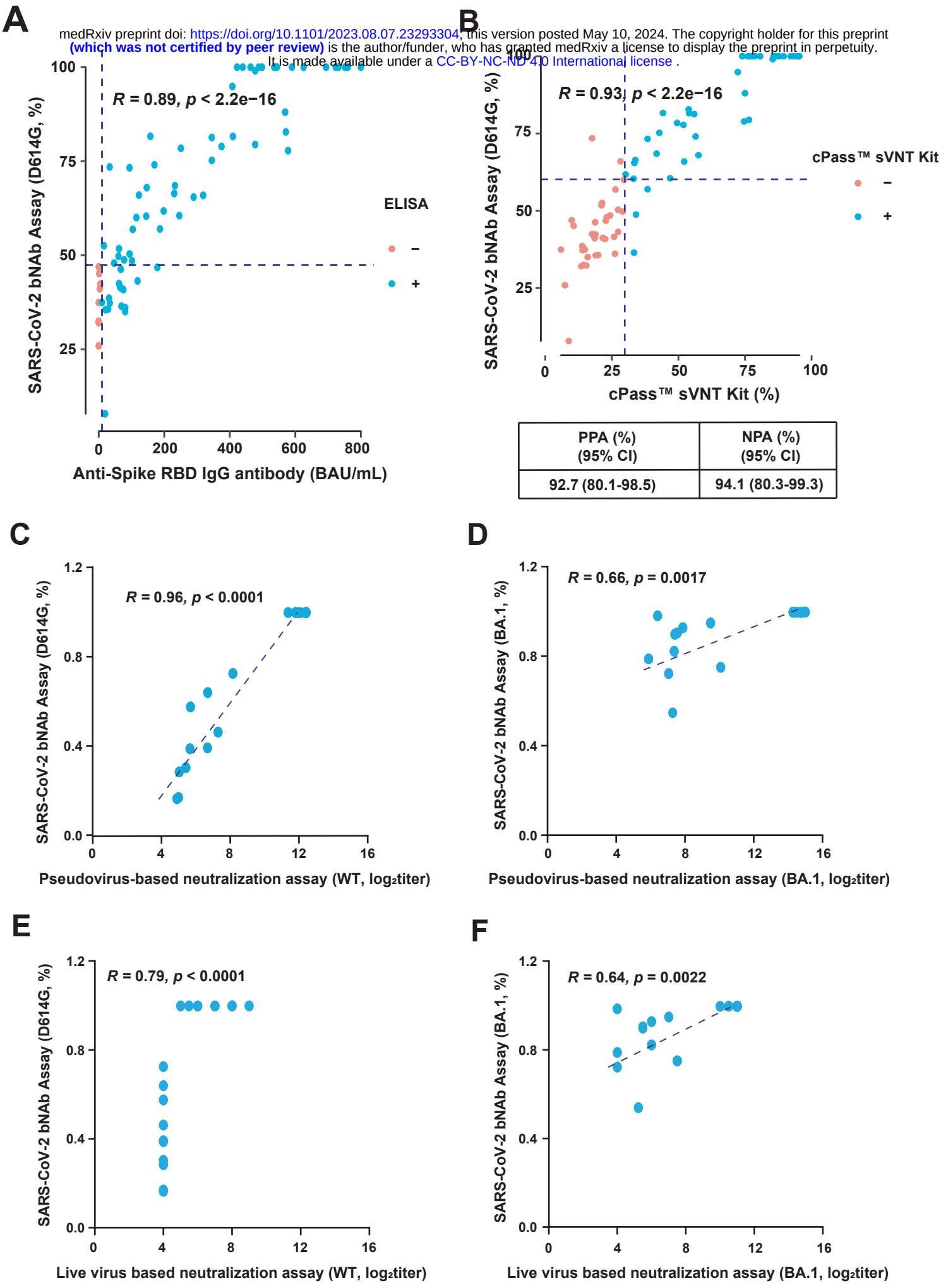

PPA (%) (95% CI)	NPA (%) (95% CI)
92.7 (80.1-98.5)	94.1 (80.3-99.3)

Figure 4

medRxiv preprint doi: https://doi.org/10.1101/2023.08.07.23298304; this version posted May 10, 2024. The copyright holder for this preprint (which was not certified by peer review) is the author/funder, who has granted medRxiv a license to display the preprint in perpetuity. It is made available under a CC-BY-NC-ND 4.0 International license .

A

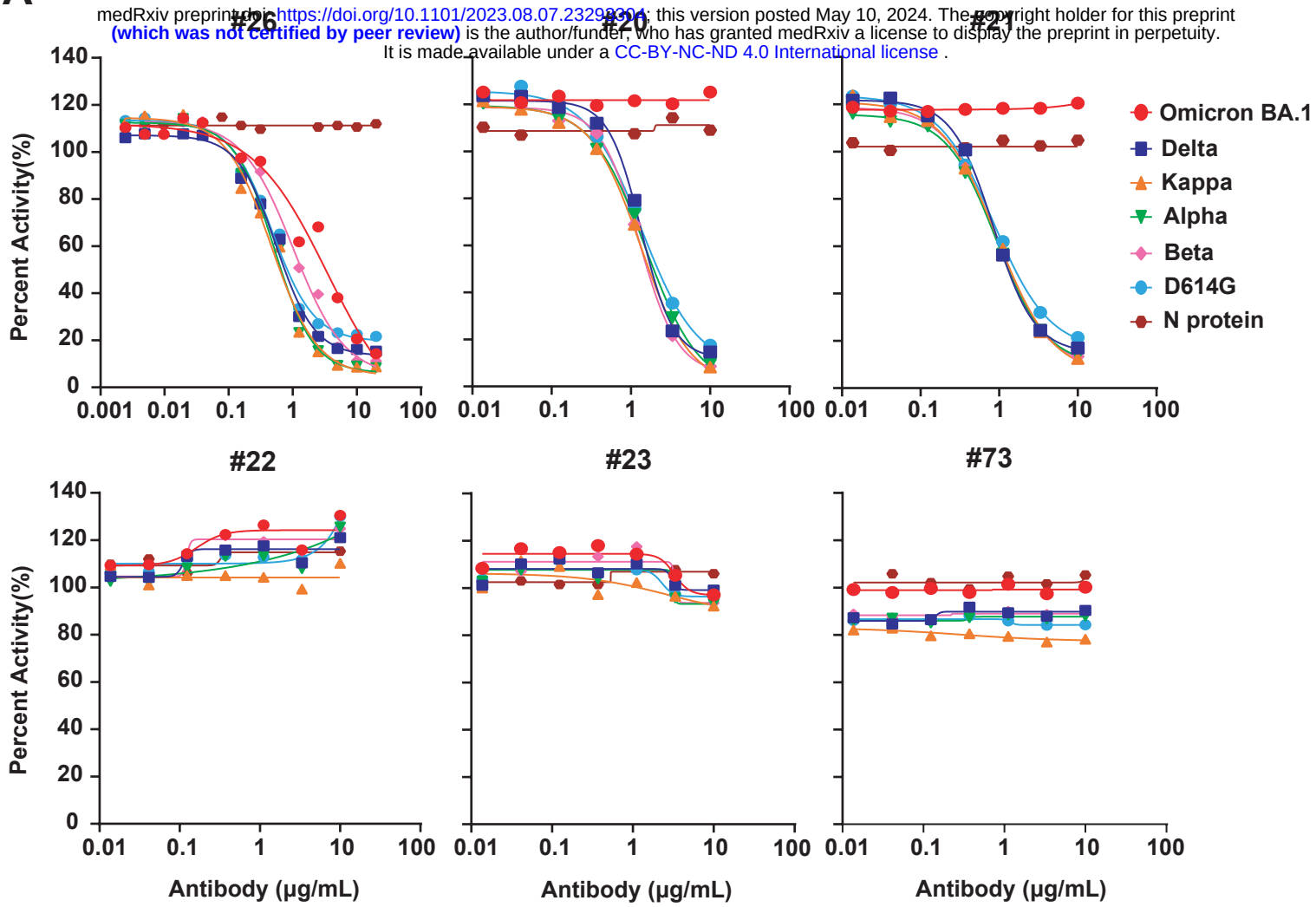

B

Antibody	D614G	Alpha	Beta	Delta	Kappa	Omicron BA.1
#26	0.4739	0.511	1.021	0.5504	0.468	3.429
#20	1.365	1.524	1.266	1.343	1.324	> 10
#21	0.8505	0.9199	0.8998	0.8429	0.9445	> 10
#22	> 10	> 10	> 10	> 10	> 10	> 10
#23	> 10	> 10	> 10	> 10	> 10	> 10
#73	> 10	> 10	> 10	> 10	> 10	> 10

IC50 (μg/mL)

0 5 10

Figure 5
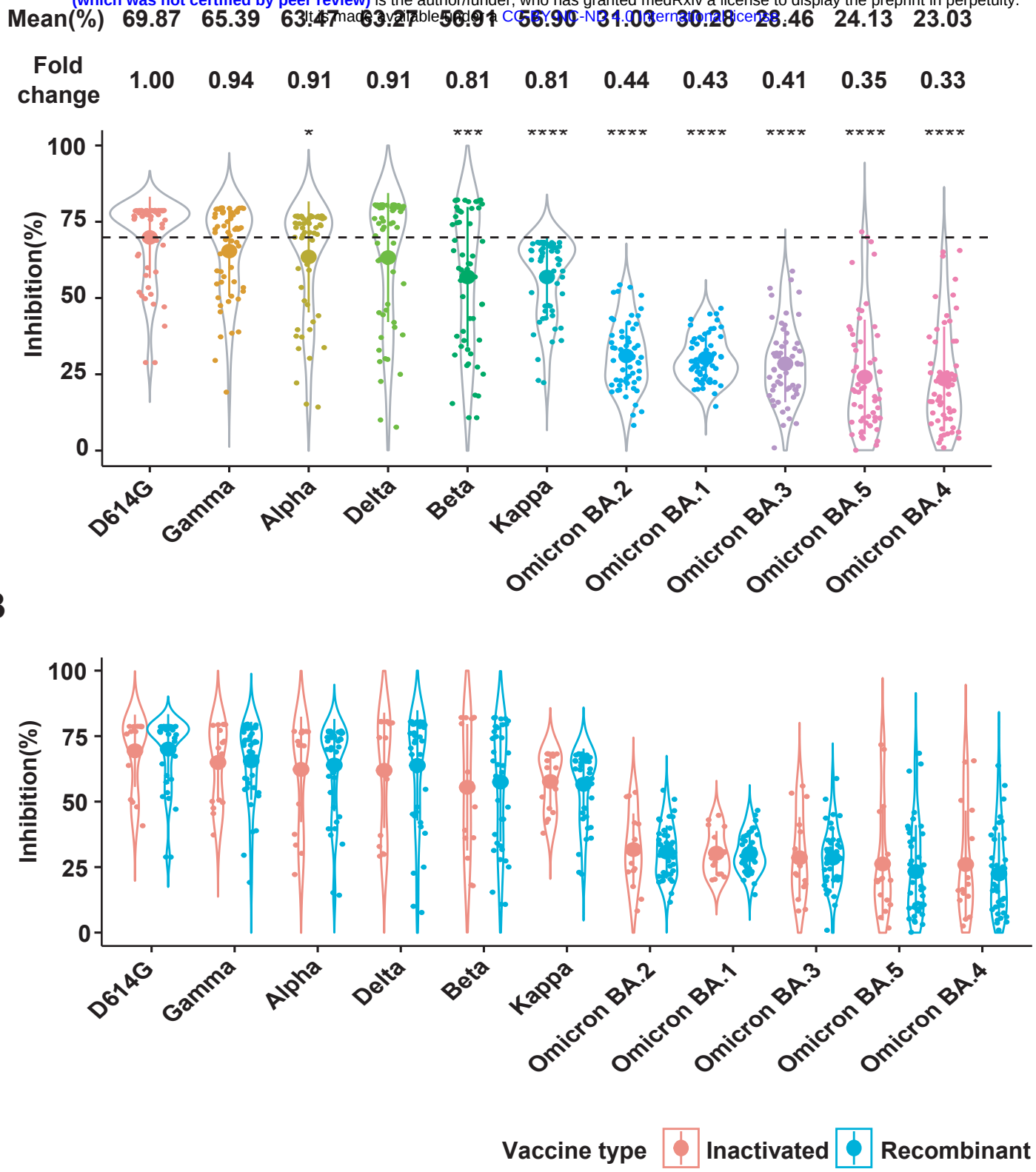
medRxiv preprint doi: https://doi.org/10.1101/2023.08.07.23293304; this version posted May 10, 2024. The copyright holder for this preprint (which was not certified by peer review) is the author/funder, who has granted medRxiv a license to display the preprint in perpetuity. It is made available under a CC-BY-NC-ND 4.0 International license.